

Dynamic behaviour of a battery pack for agricultural applications

*Original*

Dynamic behaviour of a battery pack for agricultural applications / Mocera, Francesco; Martelli, Salvatore; Costamagna, Matteo. - In: IOP CONFERENCE SERIES: MATERIALS SCIENCE AND ENGINEERING. - ISSN 1757-8981. - 1214:(2022), p. 012032. (Intervento presentato al convegno Convegno AIAS2021) [10.1088/1757-899x/1214/1/012032].

*Availability:*

This version is available at: 11583/2958222 since: 2022-03-12T08:15:01Z

*Publisher:*

IOP SCIENCE

*Published*

DOI:10.1088/1757-899x/1214/1/012032

*Terms of use:*

This article is made available under terms and conditions as specified in the corresponding bibliographic description in the repository

*Publisher copyright*

(Article begins on next page)

PAPER • OPEN ACCESS

## Dynamic behaviour of a battery pack for agricultural applications

To cite this article: F Mocera *et al* 2022 *IOP Conf. Ser.: Mater. Sci. Eng.* **1214** 012032

View the [article online](#) for updates and enhancements.

You may also like

- [The Impact of Forward Tractor Speed and Depth of Ploughing in Some Soil Physical Properties](#)

A. N. N. Kakahy, W. F. A. Alshamary and A. A. Kakei

- [Wheeled tractors in the agricultural machine-tractor aggregates work efficiency opportunities](#)

D D Nekhoroshev, D A Nekhoroshev, P V Konovalov et al.

- [Investigation of the damping properties of the process module for a tractor of traction class 1.4](#)

M V Sidorov, I P Troyanovskaya, V A Sokolova et al.



The Electrochemical Society  
Advancing solid state & electrochemical science & technology

242nd ECS Meeting

Oct 9 – 13, 2022 • Atlanta, GA, US

Abstract submission deadline: **April 8, 2022**

Connect. Engage. Champion. Empower. Accelerate.

**MOVE SCIENCE FORWARD**



Submit your abstract



# Dynamic behaviour of a battery pack for agricultural applications.

F Mocera<sup>1</sup>, S Martelli<sup>1</sup> and M Costamagna<sup>1</sup>

<sup>1</sup>Politecnico di Torino, Department of Mechanical and Aerospace Engineering, Corso Duca degli Abruzzi 24, 10129 Torino, Italy

E-mail: [francesco.mocera@polito.it](mailto:francesco.mocera@polito.it)

**Abstract.** Fight and contrast against climate change and global warming can be considered the most important challenge for the next decades. One of the most involved sectors is the one related to the carriage of passengers and goods, and, recently, also the work vehicles too. The agricultural machines and tractors are no exception to this. Indeed, agricultural industry is the second contributor in terms of pollutant emissions. So, research about agricultural machinery is focusing itself about the development of more sustainable propulsion systems such as hybrid or full-electric solutions. One of the most important components of a hybrid or full electric vehicle is the battery pack. The lack of adequate vibration isolation is the main cause of battery pack failure during operation. In the field of the agricultural vehicles, since the maximum speed is quite low and the weight of the various subsystems are high, combined with heavy working cycles, the dynamic analysis of the battery pack focuses on its low frequency behaviour. In this context, this paper focuses the attention on the dynamic behaviour of a battery pack, thought for a plug-in hybrid electric orchard tractor, through simulations obtained taking advantage of FEM and multibody software. In particular, it will be illustrated the dynamic behaviour of the battery pack while the tractor is moving on a bumpy road and when the tractor chassis is subjected to an impulsive load.

## 1. Introduction

Recently, the agricultural machines field has begun to show attention to the development of hybrid-electric solutions [1]. The main problem related to the design of hybrid or electric tractors is the high overweight with respect to the traditional ICE vehicles. This may cause some problems, such as high pressure on the soil, reduction of tractor's maximum speed and high energy consumption [2].

Considering agricultural machines, since vehicles speed range is quite low (the maximum vehicle speed is usually set to 40 km/h) and their weight is very high, due to heavy duty cycles during operation, the dynamic analysis of the battery pack should focus the attention on low frequencies vibrations. Usually, battery packs for electric vehicle are the result of sheet metal components assembled by bolts or welds, whose prestress due to joining may influence the battery pack dynamic response [3]. The correct design of the battery pack is very important: indeed, the main cause of battery packs long-term failure is represented by inappropriate vibration isolation. While the tractor is moving, low-frequency vertical vibrations are transmitted from the road to the vehicle. Furthermore, the presence of road irregularities such as potholes and bumps may trigger resonance phenomena [4]. For these reasons, is fundamental that battery pack natural frequencies are not included between 5 – 30 Hz. Indeed, resonance may compromise Li-Ion cells life [5] or trigger a series of exothermic reactions that may cause gas leak, fire or explosion. Thus, from the dynamic point of view, the main design goals should pursue high mechanical strength, maximum natural frequencies and optimization of the battery pack weight [6].



## 2. Case Study

The battery pack, described in this paper, is intended to be installed in a PHEV orchard tractor, according to a parallel hybrid-electric architecture [7,8]. According to this, the cells, which are contained in the accumulator, may be considered as an impulsive power source of energy [9] that takes action to help ICE engine in certain situations. The main features of an orchard tractor are the compact shape, the operation in tight space and on high slope roads. Other important characteristics of the orchard tractor are the reduced wheelbase (< 2m) and track width (< 1,6m), height less than 2,5 m and a maximum steering angle of approximately 50°. The battery pack of this case study is characterized by a nominal voltage of 640 VDC and a capacity of 16 kWh. The battery pack is constituted by 200 Li-Ion cells (electrical configuration 200s1p) subdivided in 8 modules connected in series. Each module (Figure 1.a) presents 25 Li-Ion cells (electrical configuration 25s1p). The module shape is similar to a box, whose size features are 233mm x 230mm x 270mm (height x width x depth). In addition to this, the battery pack also presents an electronic converter (EC) (Figure 1.b) which contains all the sub-systems required to guarantee battery safety and to monitor and manage the cells (BMS, relays, fuses etc.). The EC shape is substantially a box, whose size features are 500mm x 230mm x 260mm (width, height and depth). Both battery module and EC case are made of sheet metal.

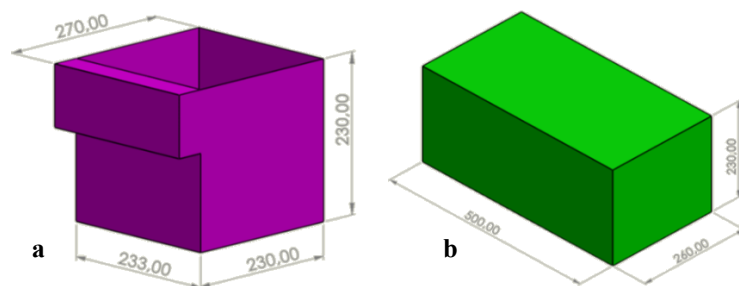


Figure 1. a) Battery module; b) Electronic converter.

Considering the battery pack location in the vehicle, while for automotive field it is well-known [10], for agricultural vehicles the battery pack location is one of the most important challenges. The main aim was to preserve the traditional tractor shape in such a way that the vehicle functionality and visibility could remain unchanged. Another goal was to achieve a high compactness level of electrical and electronic components. For these reasons, the battery pack has been placed in the area included between the cab and ICE bonnet (Figure 2).

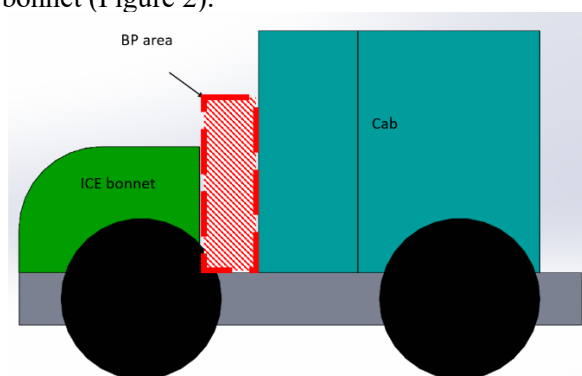
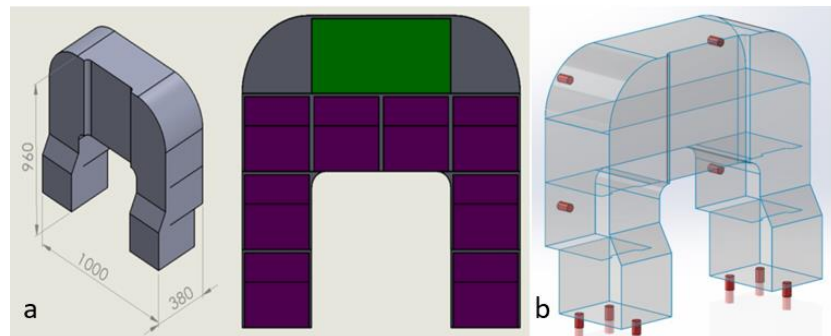


Figure 2. Battery pack location.

As consequence, the battery case presents a horseshoe shape, in which all the element mentioned before are contained (Figure 3.a). The battery case is fixed to the vehicle chassis with 10 anti-vibration supports (Figure 3.b): 6 supports fix the battery pack bases to the chassis, while the others fix the battery pack back wall.



**Figure 3.** a) battery case; b) Anti-vibration supports location.

### 2.1 FEM model

First step to model the system is the definition of its geometry. From a geometrical point of view, since all the structures are made of sheet metal, each component was realized with surface modelling technique to better represent their plane stress field while allowing for the component thickness parameterization. To complete the geometric model, there are 2 surfaces under the battery pack bottom plates, representing the chassis plates, on which the accumulator has been installed. Secondly, through the pre-processing environment, each metal sheet of every component was related with a “contact-bonded” constraint to simulate welds. The same kind of constraint was used also to simulate modules and electronic converter fastening: indeed, their bottom plate are bounded to battery pack case (Figure 4).

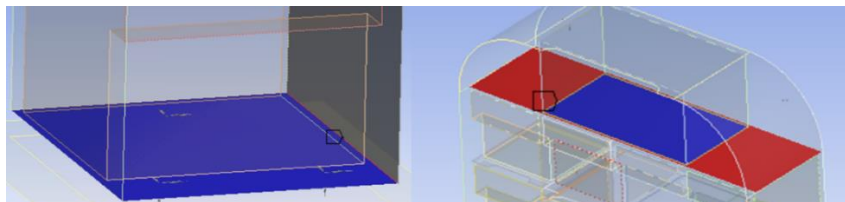


**Figure 4.** Contact constraints examples.

To simulate Li-Ion cells and safety components weight, a distributed mass of 30 kg has been applied on the bottom plates of the modules and of the EC. In this way, it was possible to well approximate the inertial properties of the system without straining computing power. The anti-vibrating supports are fixing elements and, at the same time, vibrations isolation elements. To represent this condition each anti-vibrating support was characterized by 3 orthogonal COMBIN14 spring elements (Figure 5). Each group of springs presents a longitudinal-stiffness (corresponding to the value in the catalogue) and a traverse-stiffness (corresponding to the half catalogue value).

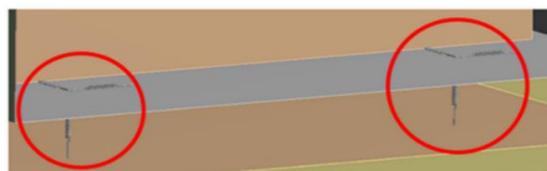


**Figure 5.** Anti-vibrating supports FEM modelling.

Concerning the meshing process, all the system components were discretized with SHELL281 elements (6 d.o.f. for each node), using “Curvature” size function. The maximum element dimension, after convergence analysis procedure, has been set to 30 mm. The result has been a homogeneous mesh grid composed by 28037 nodes and 8078 elements (Figure 6) without excessive mesh distortions.

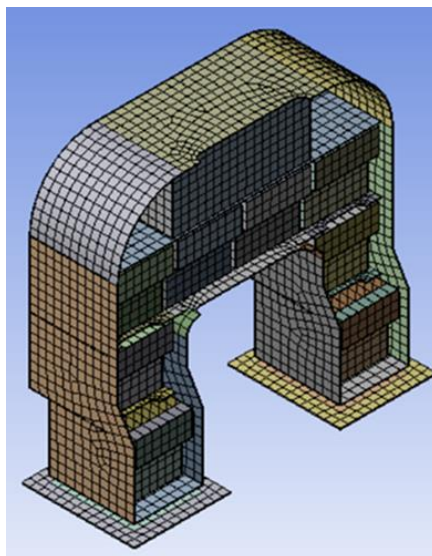


Figure 6. System discretization.

**3. Modal Analysis and overload test**

The first simulations executed to evaluate the dynamic behaviour of the system were the modal analysis and the overload test. The observation of the system natural frequencies is fundamental to avoid resonance phenomena. Focusing on the battery pack system, it is sufficient to have the lowest natural frequencies higher than 20-30 Hz. In this paper, the first 7 vibrating modes will be considered, as the lowest number of modes to obtain a reliable result. The overload test is important because, the tractor, during operation, may overcome an obstacle, such as a bump, at high-speed. It consists of a transient analysis, structured as shown in figure 7.



Figure 7. Impulsive load profile for overload analysis.

The system main features are shown in the following table:

Table 1. Battery pack main features.

| DATA                         | VALUE  |
|------------------------------|--------|
| Battery case walls thickness | 4 mm   |
| Modules/EC walls thickness   | 2,5 mm |
| Chassis plates thickness     | 5 mm   |
| Damping Factor               | 3 %    |

Concerning the materials composing the different structures, 3 macro-cases has been evaluated:

**Table 2.** Macro-cases description.

| Macro-case | Battery case material | Module/EC material    |
|------------|-----------------------|-----------------------|
| 1          | S235JR (steel)        | S235JR (steel)        |
| 2          | S235JR (steel)        | EN-AW-3003 (Al alloy) |
| 3          | EN-AW-3003 (Al alloy) | EN-AW-3003 (Al alloy) |

For each macro-case 3 different kind of anti-vibrating support have been tested:

**Table 3.** Anti-vibrating supports main features.

| Thread | Stiffness (N/mm) | Max. deformation (mm) | Length (mm) | Diameter (mm) |
|--------|------------------|-----------------------|-------------|---------------|
| M12    | 1500             | 5                     | 25          | 75            |
| M12    | 2200             | 4                     | 25          | 75            |
| M12    | 3300             | 3                     | 25          | 75            |

The main aim of this simulation campaign is the research of the best anti-vibrating support and materials combination.

The designed goals set for the modal analysis and overload test are:

- Natural frequencies >20 Hz.
- Maximum allowable stress equal to 1/3 of the corresponding material yield stress.
- Maximum vertical deformation equal to 5 mm.
- No interferences.
- Amplitude of oscillation of EC support plate must be < 1 mm in absolute value.

The amplitude of oscillation of the EC support, considered 1 side node and 1 central node of the EC support plate, has been evaluated in this way:

$$\text{Amplitude}(t) = v_{\text{centralnode}}(t) - v_{\text{sidenode}}(t) \quad (1)$$

Where:

- Amplitude: amplitude of oscillation as a function of time expressed in mm.
- $u_{\text{bdnsq kmcd}}$ : vertical deformation of the central node of the EC support plate (Figure 8).
- $u_{\text{rlc dmc d}}$ : vertical deformation of the side node of the EC support plate (Figure 8).

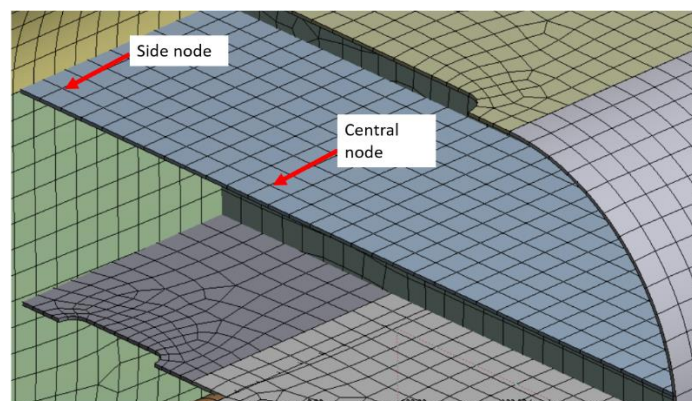


**Figure 8.** Node selected for amplitude of oscillation study.

All the simulations did not consider the damping coefficient of the anti-vibrating support, because the support damping factor is extremely complex to model (elastomeric material, non-linear behaviour, lack of a strong theoretical basis). Furthermore, this choice fitted well in a design logic according to the worst-case principle.

### 3.1 Result discussion

The results obtained from the modal analysis (Figure 9) showed that:

- Increasing anti-vibrating support stiffness, the natural frequencies grow.
- Using same-stiffness anti-vibrating supports, if the density and stiffness of the material used decrease, the natural frequencies of the modes that describe a global behaviour of the system grow.
- Using same-stiffness anti-vibrating supports, if the density and stiffness of the material used decreases, the natural frequencies reduce themselves, when the corresponding vibration mode describes a local phenomenon.

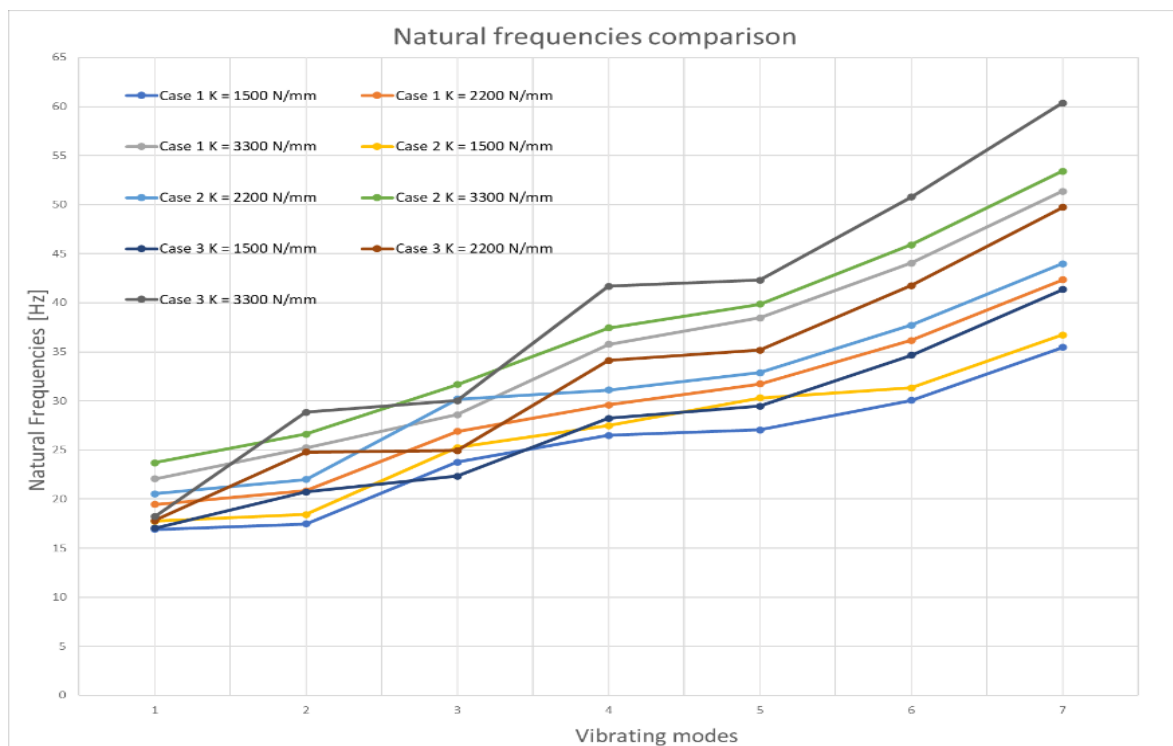


Figure 9. Natural frequencies comparison.

The results of the overload test are shown in the following table:

Table 4. Overload test results.

| Macro-Case 1             |                       |                         |                     |         |              |             |               |           |
|--------------------------|-----------------------|-------------------------|---------------------|---------|--------------|-------------|---------------|-----------|
| Support stiffness (N/mm) | $\sigma_{Case}$ (MPa) | $\sigma_{module}$ (MPa) | $\sigma_{EC}$ (MPa) | SF Case | SF module/EC | V_Case (mm) | V_module (mm) | V_EC (mm) |
| 1500                     | 80,88                 | 28,99                   | 28,91               | 2,91    | 8,13         | 5,84        | 5,45          | 5,79      |
| 2200                     | 85,34                 | 27,88                   | 31,24               | 2,75    | 7,52         | 4,17        | 3,82          | 4,12      |
| 3300                     | 89,88                 | 29,33                   | 29,03               | 2,61    | 8,01         | 3,2         | 2,87          | 3,16      |

Macro-Case 2

| Support stiffness (N/mm) | $\sigma_{Case}$ (MPa) | $\sigma_{module}$ (MPa) | $\sigma_{EC}$ (MPa) | SF Case | SF module/EC | V_Case (mm) | V_module (mm) | V_EC (mm) |
|--------------------------|-----------------------|-------------------------|---------------------|---------|--------------|-------------|---------------|-----------|
| 1500                     | 70,01                 | 19,964                  | 12,99               | 3,36    | 8,26         | 5,60        | 5,34          | 5,56      |
| 2200                     | 67,83                 | 19,416                  | 12,438              | 3,46    | 8,50         | 3,93        | 3,89          | 3,75      |
| 3300                     | 99,35                 | 20,7                    | 20,483              | 2,37    | 7,97         | 3,5         | 2,88          | 3,45      |

Macro-Case 3

| Support stiffness (N/mm) | $\sigma_{Case}$ (MPa) | $\sigma_{module}$ (MPa) | $\sigma_{EC}$ (MPa) | SF Case | SF module/EC | V_Case (mm) | V_module (mm) | V_EC (mm) |
|--------------------------|-----------------------|-------------------------|---------------------|---------|--------------|-------------|---------------|-----------|
| 1500                     | 81,59                 | 29,32                   | 19,83               | 2,02    | 5,63         | 6,88        | 5,43          | 6,77      |
| 2200                     | 87,79                 | 31,86                   | 15,72               | 1,88    | 5,18         | 4,86        | 4,35          | 4,78      |
| 3300                     | 92,58                 | 36,64                   | 13,4                | 1,78    | 4,50         | 3,35        | 3,48          | 3,26      |

The transient analysis showed that:

- Increasing the mass of the system, using same stiffness anti-vibrating supports, the maximum vertical deformation reduces itself.
- In every single sub-case, the average stress is very low (less than 10 MPa), while the peak values are recorded during the load application phase.
- The modules and the electronic converter are characterized by very low stress value.
- The maximum stressed areas are the EC support plate and the internal connection zone (Figure 10).
- In general, the EC support plate oscillation is similar for each case, and it is less than 1 mm almost for each sub-case (Figure 11).

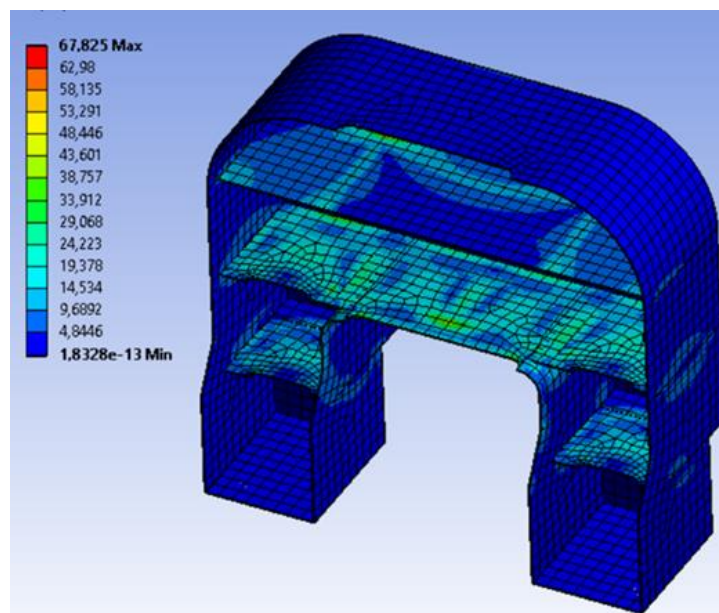
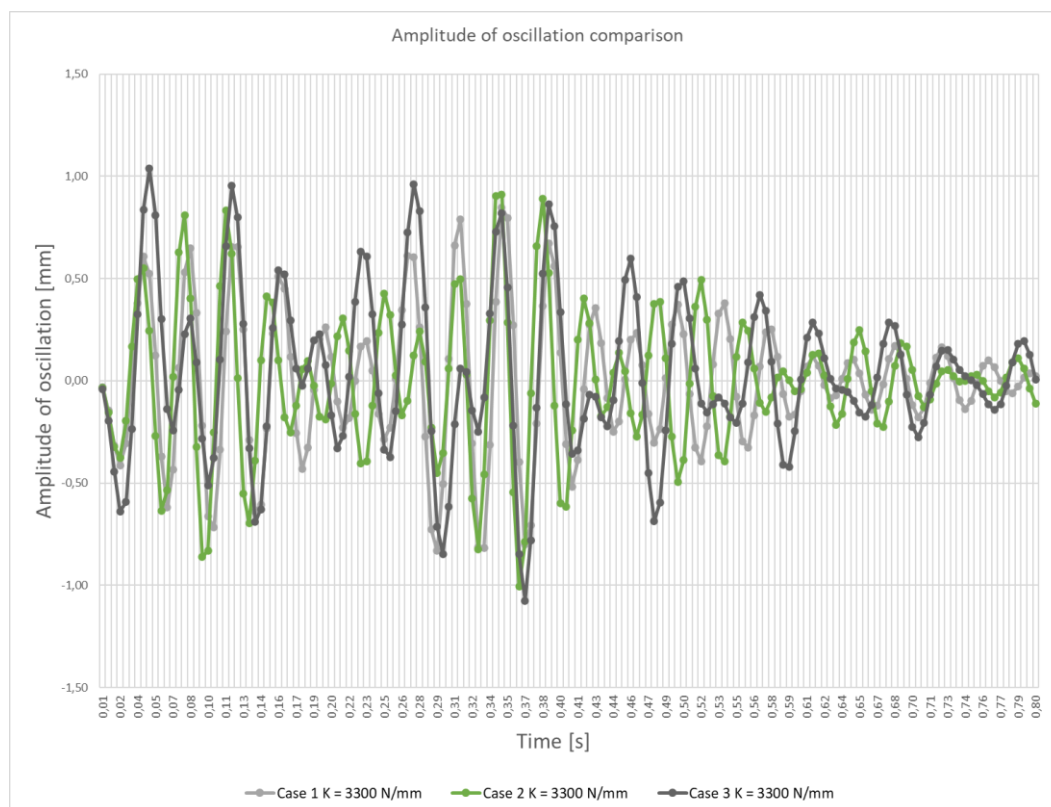


Figure 10. Macro-case 2,  $K = 2200$  N/mm, stress distribution.



**Figure 11.** EC support plate Amplitude of oscillation comparison.

Most of the impulsive load is absorbed by the battery case structure, securing the modules and the EC. As said before, the main aim of these simulations has been the research of the best combination structures materials – anti-vibrating support. Only one combination achieved all the design goals: Macro-case 2 (battery case made of S235JR steel and modules and the electronic converter made of EN-AW 3003) using anti-vibrating supports with stiffness  $K = 2200$  N/mm. However, also macro-case 2 and anti-vibrating supports with stiffness  $K = 3300$  N/mm showed very interesting results, especially some improvements of the system geometry. In conclusion, following the results obtained in this simulation campaign, the battery pack was characterized by a good dynamic response to an impulsive load.

### 3.2 Improved model

What has been described until now represents the basic model of the battery pack. To improve the dynamic behaviour of the system, some changes has been implemented. In particular, the updates consist of:

- Addition of 2 ribs on the EC support plate (Figure 12).
- Battery case cover thickness reduced from 4 to 3 mm.
- Modules and EC walls thickness reduced from 2,5 to 2 mm.

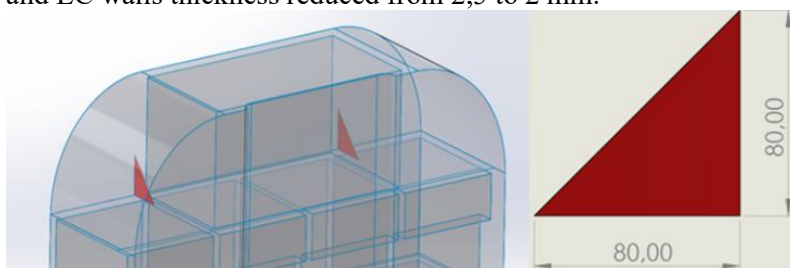


**Figure 12.** Ribs added to the model.

So, the improved model has been subjected to the same tests done for the basic model. In this case, the combination anti-vibrating support – structural materials used are the macro-case 2 and support stiffness  $K = 2200 \text{ N/mm}$  and  $K = 3300 \text{ N/mm}$ . The results of the modal analysis are illustrated in the following figure:

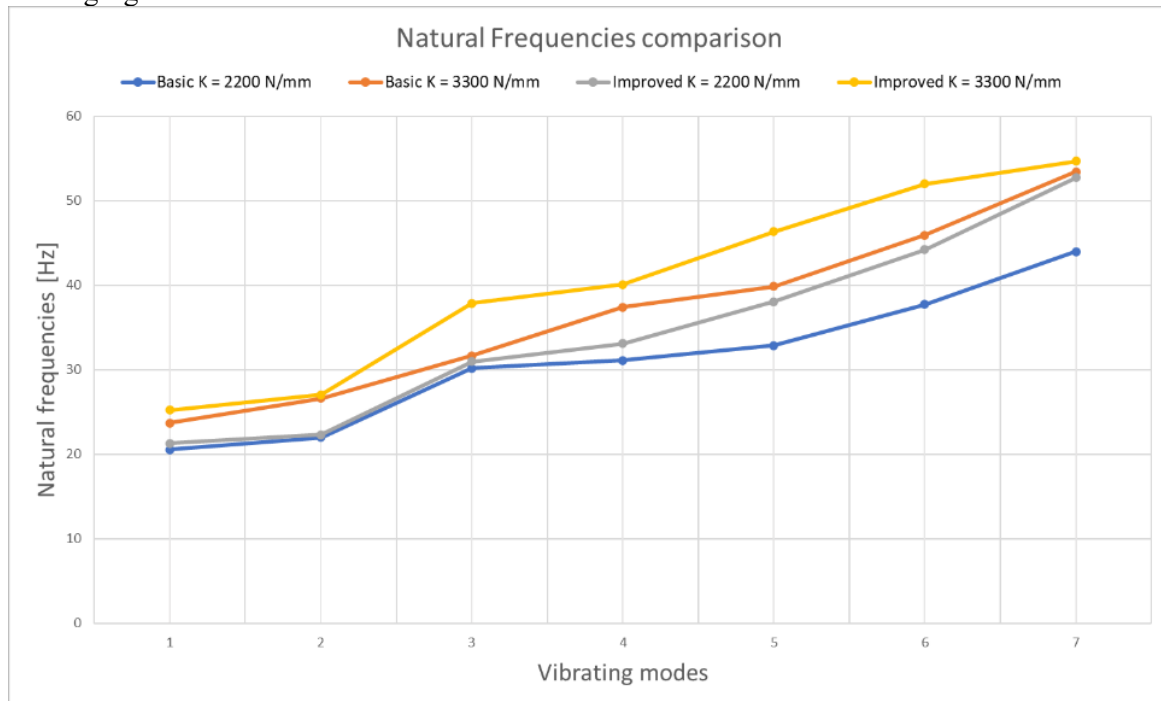


**Figure 13.** Natural Frequencies comparison between basic and improved model.

Observing fig. 13, going from the basic model to the improved one, the natural frequencies of the system grow. Considering the vibrating modes with the highest modal participation factor (Figure 14), there is an increment of 3,6% ( $K = 2200 \text{ N/mm}$ ) and 6,4% ( $K = 3300 \text{ N/mm}$ ) for the mode “a”, and an increment of 46% ( $K = 2200 \text{ N/mm}$ ) and 64% ( $K=3300 \text{ N/mm}$ ) for the mode “b”.

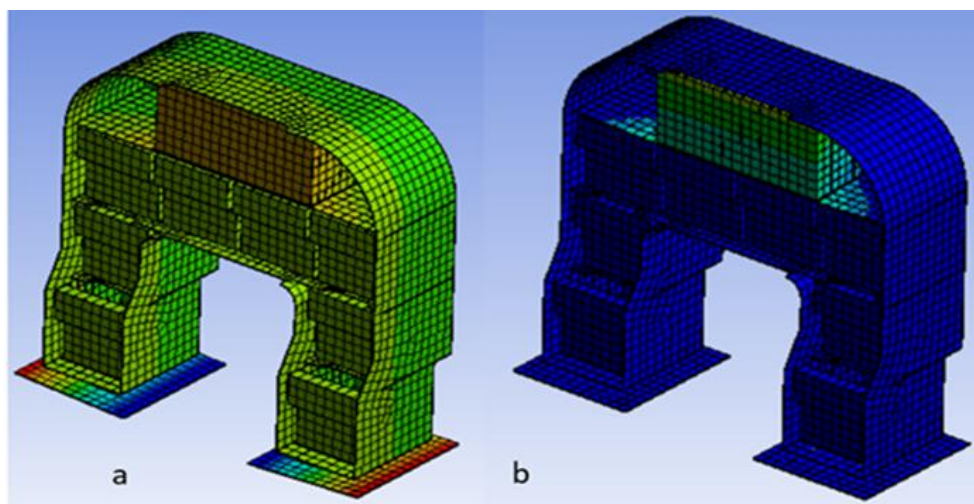


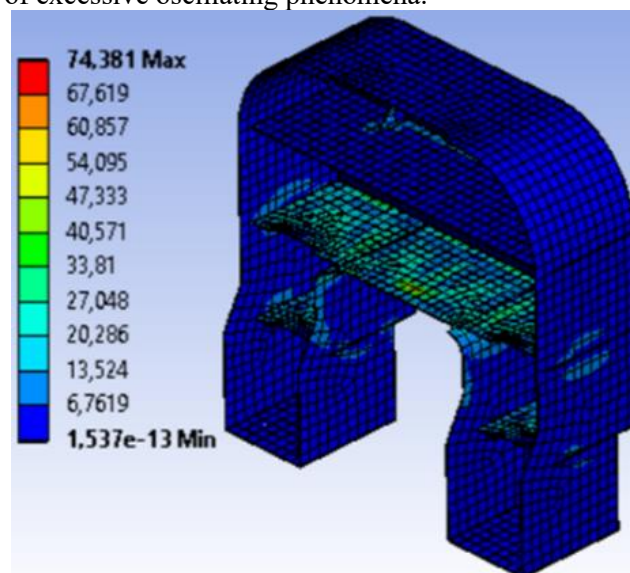
**Figure 14.** Vibrating modes with the highest participation factor.

The reasons that can explain this improvement are the system weight reduction (- 10%) and the presence of the ribs on the EC support plate. The results of the overload test are shown in the following table:

**Table 5.** Overload test result and comparison between basic and improved model.

| Support stiffness (N/mm) | $\sigma_{Case}$ (MPa) | $\sigma_{module}$ (MPa) | $\sigma_{EC}$ (MPa) | SF Case | SF module/EC | V_Case (mm) | V_module (mm) | V_EC (mm) |
|--------------------------|-----------------------|-------------------------|---------------------|---------|--------------|-------------|---------------|-----------|
| 2200 Basic               | 67,83                 | 19,42                   | 12,44               | 3,46    | 8,50         | 3,93        | 3,89          | 3,75      |
| 3300 Basic               | 99,35                 | 20,7                    | 20,48               | 2,37    | 7,97         | 3,5         | 2,88          | 3,45      |
| 2200 Improved            | 65,26                 | 23,5                    | 5,64                | 3,6     | 7,02         | 3,68        | 3,7           | 3,55      |
| 3300 Improved            | 74,4                  | 26,05                   | 4,99                | 3,16    | 6,33         | 2,91        | 2,99          | 2,87      |

Observing *table 5* it is evident the reduction of the maximum stress on the battery case structure: indeed, considering anti-vibrating support with stiffness  $K = 3300$  N/mm, there is a reduction about 25 % respect to the basic model. Furthermore, the entire system is not subject to an intense field of stress with an average stress recorded less than 5 MPa. The most stressed area is the internal connection zone (Figure 15), while the EC support plate, thanks to the presence of the ribs, is not much stressed anymore (maximum stress recorded 40 MPa). Also, for the improved model, almost all the impulsive load is absorbed by the battery case structure. Concerning the maximum vertical deformation, the result obtained for the improved models are better than the corresponding of the basic one. Furthermore, the values obtained for battery case, modules and electronic converter are very similar to each other, confirming the absence of excessive oscillating phenomena.

**Figure 15.** Stress distribution improved model  $K = 3300$  N/mm.

Concerning about the EC support plate amplitude of oscillation, observing figure 16, it is clear the advantage brought by the ribs: indeed, the reduction of the amplitude of oscillation is about 76% respect to the basic model. Considering these results, each sub-case shows a good dynamic behaviour, and all the design goals are achieved. However, the best performance is obtained with support stiffness  $K = 3300$  N/mm, so these kinds of supports will be used for the next step: the Virtual Field Test.

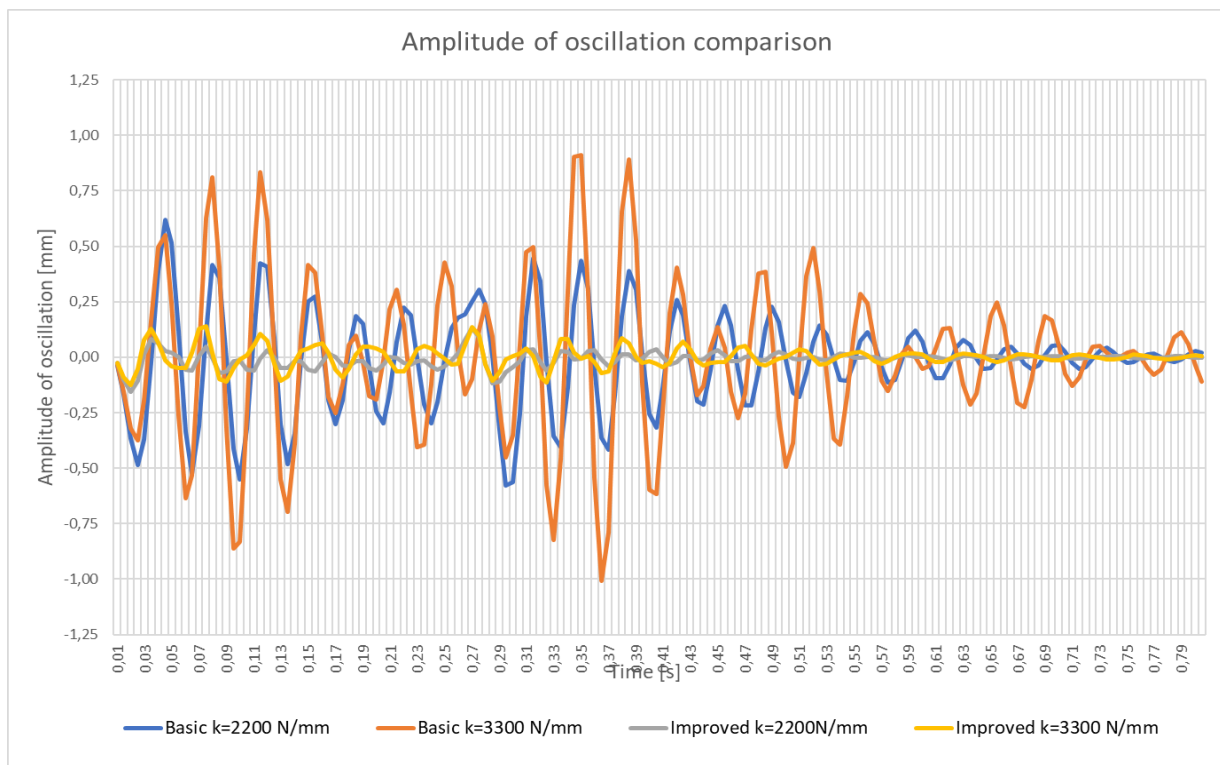


**Figure 16.** Amplitude of oscillation comparison between basic and improved model.

#### 4. Virtual Field Test

The purpose of the virtual field test is to evaluate the dynamic behaviour of the battery pack, with respect to the entire vehicle, during hard work condition situations. The aim is to replicate what happens during a real Field Test [11]. These tests are based on experience for lack of tests standardization and because they must take into account the available computing power. The virtual field tests are born combining Multibody analysis and FEM simulations. In particular, the multibody model was used to obtain a series of load profiles, applied to the battery pack's supports. Then, the load profiles constitute the input loads of a transient analysis, similar to the ones done in the overload tests, to evaluate the dynamic behaviour of the battery pack. The design goals set for these virtual field tests were:

- Load frequency application must not be close to system natural frequencies.
- Maximum allowable stress equal to 1/2 of the corresponding material yield stress.
- Absence of interferences.
- Relative vertical deformation between BP and chassis < 2 mm.
- EC support plate amplitude of oscillation < 1 mm.

##### 4.1 Virtual prototype

The virtual prototype consists of a series of rigid bodies, connected to each other with different kind of joint to limit their degrees of freedom. As said before, the tractor, described in this paper, is an orchard tractor. Dimensional and mass data are illustrated in table 6 and table 7.

**Table 6.** Dimensional data orchard tractor.

| Data      | Value   |
|-----------|---------|
| Wheelbase | 2265 mm |
| Length    | 3740 mm |

|                  |                          |
|------------------|--------------------------|
| Width            | 1536 mm                  |
| Track width      | 1216 mm                  |
| Maximum height   | 2100 mm                  |
| Ground clearance | 326,3 mm                 |
| Height at seat   | 1300 mm                  |
| ICE Dimensions   | 759 mm x 571 mm x 806 mm |
| Tyre             | 320/70 R20               |
| Transmission     | 4WD                      |

**Table 7.** Weight data orchard tractor.

| Component                       | Mass (kg) |
|---------------------------------|-----------|
| Chassis                         | 255       |
| Front and rear axle             | 180       |
| Gearbox                         | 150       |
| Transmission                    | 250       |
| ICE and bonnet                  | 745       |
| Tyres                           | 200       |
| Driver and on-board instruments | 200       |
| Battery Pack                    | 400       |
| Electric motor                  | 30        |
| Chassis internal masses         | 200       |
| Axles internal masses           | 150       |
| Total MASS                      | 2760      |

Concerning the torque regulation, it is based on vehicle speed target, and it is characterized by asymptotic behaviour. The asymptote corresponds to the maximum transmissible torque by the wheels to the ground and this limit is set to:

- 1000 Nm for each tyre in case of high-speed transmission mode.
- 2500 Nm for each tyre in case of slow-speed transmission mode.

Diesel combustion energy and battery pack are constrained to the chassis with *fixed joints*, while cab and wheels are bounded to the chassis with *bushing joints*. So, in this way the model can take into account the deformability of the tyres and of the ground too [12,13]. Finally, two markers have been positioned in correspondence to the chassis plates on which the battery pack is installed. In this way the value of the load transmitted to the battery pack from the chassis can be obtained and used to the FEM transient analysis.

#### 4.2 Virtual Field Test 1 & 2

In the first two virtual field test, the tractor is moving through a bumpy road formed by 10 speed bumps, distant 2 meters from each other. Each speed bump presents an arc of circumference shape. The main features of a single speed bump are showed in Figure 17:

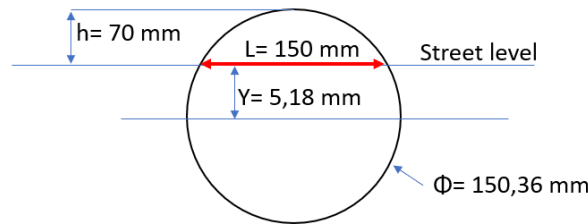


Figure 17. Virtual Field Test 1 & 2 Bump description.

The tractor is moving at 10 km/h, in slow-speed transmission configuration. Furthermore, since the aim of these tests is the simulation of an working condition, at the vehicle back end, a lumped mass of 1000 kg, simulating the rear attached implement, was positioned. The difference between virtual field test 1 & 2 (Figure 18) is that the second test presents each speed bump cut in two and every single half-part is distanced of 1 metre to the other one.

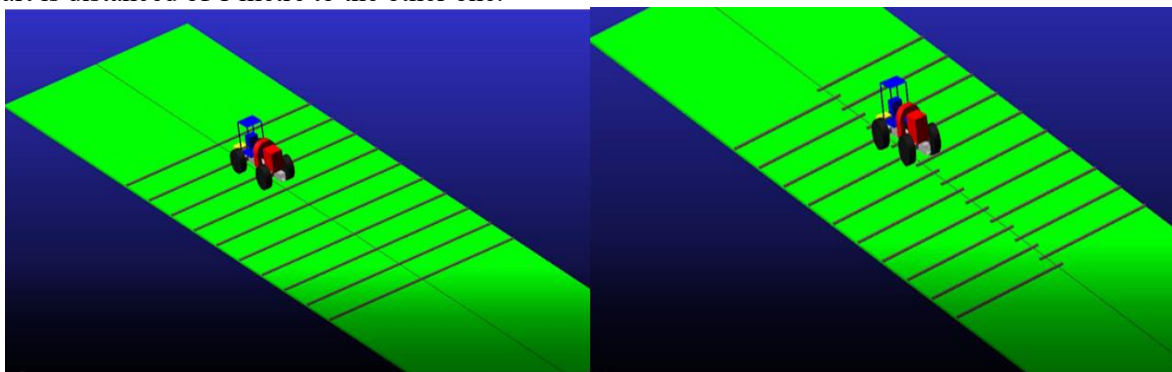


Figure 18. Virtual field test 1 (on the left) and 2 (on the right).

The results of the multibody simulation, that constitutes the input for FEM transient analysis are shown in the following figures:



Figure 19. Results multibody simulation Test 1.

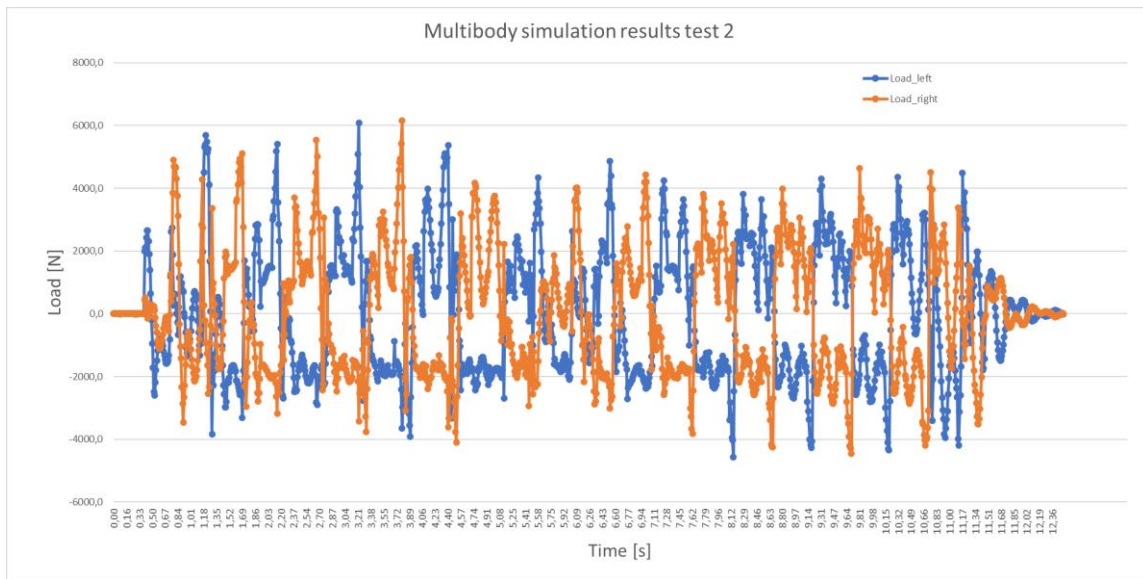


Figure 20. Results multibody simulation Test 2.

4.3 Virtual Field Test 3 & 4

In the last two field tests, the tractor is moving through a bumpy road formed by 10 speed bumps, distant 2 meters from each other. Each speed bump presents an arc of circumference shape. The main features of a single speed bump are showed in figure 21:

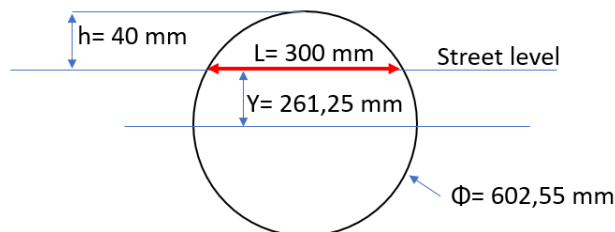


Figure 21. Virtual Field test 3 & 4 Bump description.

The tractor is moving at 30 km/h, in fast-speed transmission configuration. The difference between virtual field test 3 & 4 (Figure 22) is that the second test presents each speed bump cut in two and every single half-part is distanced of 1 metre to the other one.

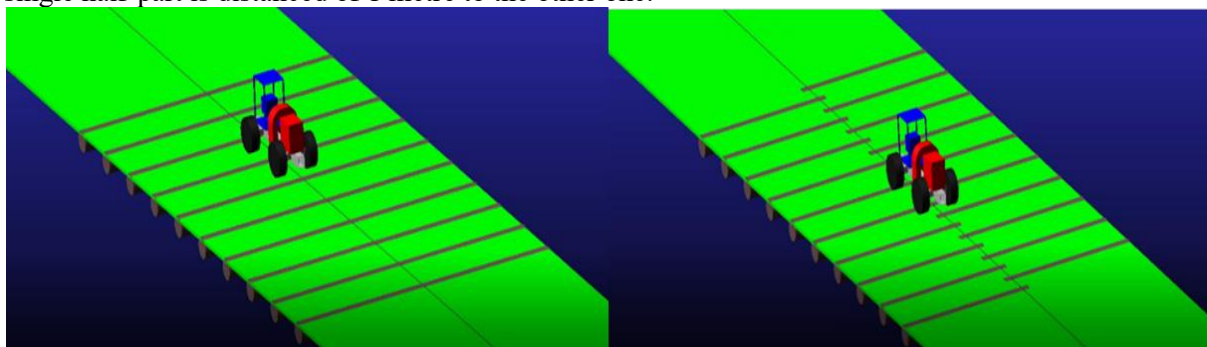


Figure 22. Virtual Field Test 3 (on the left) and 4 (on the right).

The results of the multibody simulation, that constitutes the input for FEM transient analysis are shown in the following figures:

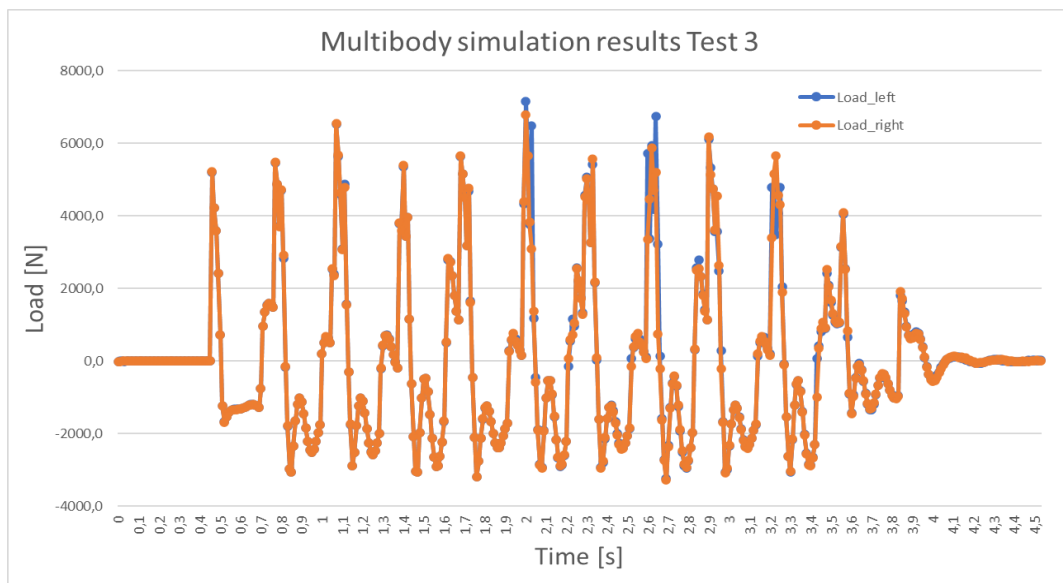


Figure 23. Results multibody simulation Test 3.

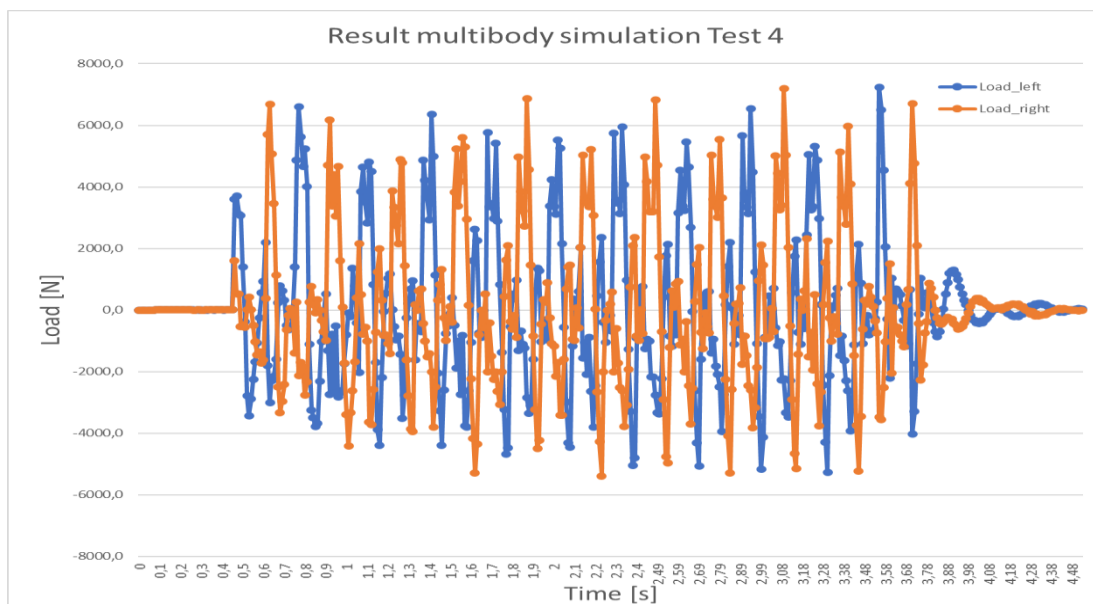


Figure 24. Results multibody simulation Test 4.

4.4 Virtual Field Tests results discussion

Table 8. Overall results Virtual Field Tests.

| Field Test   | 1      | 2      | 3       | 4       |
|--|--------|--------|---------|---------|
| Load application frequency                           | 1,4 Hz | 2,8 Hz | 4,2 Hz  | 8,33 Hz |
| Minimum SF encountered                               | 3,6    | 3      | 2,5     | 2,1     |
| Relative vertical deformation between BP and chassis | 1,2 mm | 0,6 mm | 1,6 mm  | 0,9 mm  |
| Amplitude of oscillation EC support plate            | 0,4 mm | 0,5 mm | 0,55 mm | 0,8 mm  |
| Interference   | No     | No     | No      | No      |

Table 8 shows that all the design goals are achieved, so the battery pack thought for this application has a quite positive response to heavy working conditions. Considering load application frequency, it is clear that the orchard tractor battery pack is subjected to low frequency working conditions, confirming that the frequency working range of the tractor are lower than 30 Hz. Another remarkable point is the correlation between load frequency application and stress level developed: indeed, if the frequency grows, the safety factor decreases. The highest stress level occurs during virtual field test 3 and 4. So, the most critical conditions are ruled by vehicle speed (consequently the frequency) rather than speed bump shape and dimension. The minimum Safety factor encountered is related to the battery case structure, while modules and electric converter shows a minimum safety factor upper to 10. So, even in this case almost all the input load is absorbed by the external structure of the battery case. In almost all cases, the most stressed component (Figure 25) is the EC support plate, but its amplitude of oscillation is very low thanks to the ribs presence.

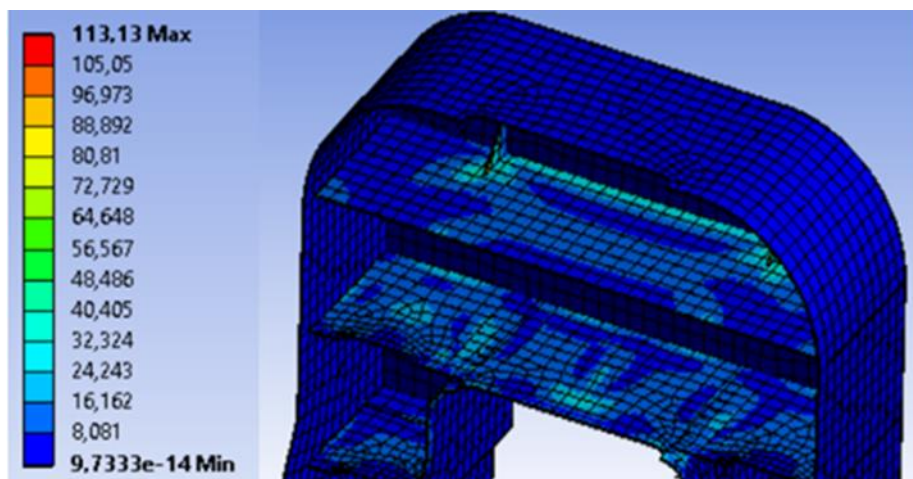


Figure 25. Stress distribution Virtual Field Test 4.

Considering relative vertical deformation between battery pack and chassis, it appears that the anti-vibrating support (quale in definitiva) are appropriate for this kind of application because the maximum allowable value is never overcome.

## 5 Conclusions

This paper shows how, even for agricultural applications, a battery pack influences dynamic behaviour, weight, and architecture of an orchard tractor. Indeed, the battery pack is an important component, not only in terms of performance, but also in terms of safety and preservation of the driver and the entire vehicle too. For these reasons, an appropriate dynamic design of the accumulator is crucial. The most important result obtained from this paper is that is possible to install, from a dynamic and mechanical point of view, a big size battery pack, in a small size tractor, as the orchard tractor, preserving its traditional shape and functionality. The most critical design goals to achieve are:

- Low natural frequencies.
- High mechanical stresses, near the yield value.

So, the main design aspects, to pay attention to, are:

- System mass.
- Structure stiffness.
- Mechanical strength.

Concerning the structural material choice, it must be the result of the best compromise in terms of:

- Mechanical strength.
- Easy manufacture.

- Low cost.

The structure stiffness must be as much high as possible to guarantee higher natural frequencies and avoid resonance phenomena. The most important contribute to stiffness structure is given by the anti-vibrating supports. Anyway, stiffening local intervention are recommended (as mechanical ribs) in strategic point of the structure too (for example in presence of cantilevered masses).

The mass of the system is fundamental, and it must be as low as possible to improve vehicle performance and dynamic behaviour because the system mass has a strong impact on natural frequencies and inertial proprieties of the structure.

This work is open to some possible improvements such as considering the non-linear spring characteristic of the anti-vibrating support to better approximate its behaviour. Another possible improvement may be the use of input data which come from real field test. Finally, this paper can be considered as the starting point to configure a complete system fatigue study.

## References

- [1] Somà A 2017 Trends and Hybridization Factor for Heavy-Duty Working Vehicles *Hybrid Electric Vehicles* (InTech)
- [2] Sitompul J, Zhang H, Noguchi R and Ahamed T 2019 Optimization study on the design of utility tractor powered by electric battery *IOP Conference Series: Earth and Environmental Science* **355**
- [3] Hong S-K, Epureanu B I and Castanier M P 2014 Parametric reduced-order models of battery pack vibration including structural variation and prestress effects *Journal of Power Sources* **261**
- [4] Arora S, Shen W and Kapoor A 2016 Review of mechanical design and strategic placement technique of a robust battery pack for electric vehicles *Renewable and Sustainable Energy Reviews* **60**
- [5] Mocera F, Soma A and Clerici. D 2020 Study of aging mechanisms in lithium-ion batteries for working vehicle applications *2020 Fifteenth International Conference on Ecological Vehicles and Renewable Energies (EVER)* (IEEE)
- [6] Shui L, Chen F, Garg A, Peng X, Bao N and Zhang J 2018 Design optimization of battery pack enclosure for electric vehicle *Structural and Multidisciplinary Optimization* **58**
- [7] Mocera F and Somà A 2021 A Review of Hybrid Electric Architectures in Construction, Handling and Agriculture Machines *New Perspectives on Electric Vehicles [Working Title]* (IntechOpen)
- [8] Mocera F and Somà A 2020 Analysis of a Parallel Hybrid Electric Tractor for Agricultural Applications *Energies* **13**
- [9] Warner J 2015 Battery Pack Design Criteria and Selection *The Handbook of Lithium-Ion Battery Pack Design* (Elsevier)
- [10] Sankaran G and Venkatesan S 2021 Standardization of electric vehicle battery pack geometry form factors for passenger car segments in India *Journal of Power Sources* **502**
- [11] Renius K T 2020 Tractor Tests *Fundamentals of Tractor Design* (Cham: Springer International Publishing)
- [12] Nicolini A, Mocera F and Somà A 2019 Multibody simulation of a tracked vehicle with deformable ground contact model *Proceedings of the Institution of Mechanical Engineers, Part K: Journal of Multi-body Dynamics* **233**
- [13] Mocera F, Somà A and Nicolini A 2020 Grousers Effect in Tracked Vehicle Multibody Dynamics with Deformable Terrain Contact Model *Applied Sciences* **10**